Shannon T. Krauss
Thomas P. Forbes
Jeffrey A. Lawrence
Greg Gillen
Jennifer R. Verkouteren

National Institute of Standards and Technology, Gaithersburg, Maryland 20899, USA

Received February 7, 2020
Revised June 4, 2020
Accepted June 10, 2020

Research Article

Detection of fuel-oxidizer explosives utilizing portable capillary electrophoresis with wipe-based sampling

Portable analytical instrumentation that can provide an alarm indication for the presence of explosives and related components is critical for the identification of explosives-based hazards and threats. Many explosives incident reports involve an inorganic oxidizer-fuel mixture which can include pyrotechnics, fireworks, flash powders, black powders, black powder substitutes, and improvised or homemade explosives. A portable CE instrument with targeted analysis of common inorganic oxidizer ions, for example, chlorate, perchlorate, and nitrate, was used here as a rapid detection platform. Unlike frequently used gas-phase separation and detection instrumentation such as ion mobility spectrometry (IMS), an automated liquid extraction mechanism is required for CE separation using acetate paper sample collection wipes. Target inorganic oxidizers were inkjet-printed onto sample wipes to investigate instrument response relative to the collected analyte spatial distribution. Overall, analyte signal intensities increased with off-center sample deposition due to improved sample extraction from wipes and no change in response was observed for varied array distributions across wipes. The system demonstrated sub 200 ng detection limits for all target analytes, with further improvement when normalizing to an internal standard.

Keywords:
Capillary electrophoresis / Conductivity detection / Inorganic explosives / Portable instrumentation / Wipe
DOI 10.1002/elps.202000094

Additional supporting information may be found online in the Supporting Information section at the end of the article.

1 Introduction

The prevention of potential hazards and threats relating to explosives requires deployable analytical techniques that can provide an indication, or alarm, for the presence of explosives and related components. According to the 2018 U.S. Bomb Data Center Annual Explosives Incident Report, the most common main charges reported are inorganic-based explosives, necessitating the need for targeted, high-throughput screening techniques [1]. Generally, inorganic-based explosives consist of an inorganic oxidizer and a fuel, and can encompass pyrotechnics, fireworks, flash powders, black powders (BPs), and improvised or homemade explosives. Common inorganic oxidizer salts include potassium chlorate, potassium perchlorate, potassium nitrate, and ammonium nitrate, and are oftentimes the focus of deployable detection techniques.

Employing direct chemical analysis offers advantages for high-throughput checkpoint screening due to the rapid analysis times, reduced sample handing, and elimination of solvents and wastes from sample preparatory steps [2]. Optical techniques, such as surface-enhanced Raman scattering (SERS), have sufficient sensitivity to be applied for submicrogram detection of inorganic explosives [3]. However, SERS is somewhat limited by requirements for dissolution of the analyte in nanoparticle suspensions or deposition onto thin films and metallic substrates [4]. Some groups have successfully developed flexible SERS substrates for both sample collection and direct chemical analysis using paper [5–7] and hydrogels [8]. Similar efforts for explosives detection are limited and focused on organic compounds [9].

Correspondence: Dr. Shannon T. Krauss and Dr. Thomas P. Forbes, 100 Bureau Drive, Mail Stop 8371, Gaithersburg, MD 20899.
E-mail: shannon.krauss@nist.gov; thomas.forbes@nist.gov

Abbreviations: **BP**, black powder; **BPS**, black powder substitute; **IMS**, ion mobility spectrometry; **IS**, internal standard; **SERS**, surface-enhanced Raman scattering

Color online: See article online to view Figs. 1–5 in color.

Additional screening techniques exploit the inherent vapor pressures of target explosive analytes for sample collection and analysis, for example, canines [10] and chemical "sniffers" [11]. These inherent properties can also be utilized for sample extraction from collection wipes and gas-phase analysis, for example, ion mobility spectrometry (IMS) [12]. IMS has been extensively deployed for airport and other checkpoint security worldwide. With traditional IMS, a thermal desorber is utilized to heat ($\leq$280°C) collected sample from a surface wipe to target more volatile explosive compounds, such as 2,4,6-trinitrotoluene (TNT) and cyclo-1,3,5-trimethylene-2,4,6-trinitramine (RDX), for rapid sample analysis within 10 s [13]. Although IMS is advantageous for organic explosives, detection of nonvolatile inorganic explosives is challenging due to the lower vapor pressures of refractory inorganic oxidizer components. Improvements toward inorganic-based explosives detection have focused on increasing the sensitivity for sulfur identification [14], utilizing acid-enhanced evaporation [15,16], and employing instrument modifications for reaching increased thermal desorption temperatures [17–19]. Peng et al. were able to achieve $<$10 ng sensitivities for nitrate, chlorate, and perchlorate using acid enhancement and analysis times within 5 s [15]. However, this required an additional sample pretreatment step and introduced acids to the IMS instrument. Frequently deployed screening techniques also include handheld chemical sensors utilizing colorimetric and fluorescence detection methods [10]. Although colorimetric sensors are advantageous due to the low cost, availability, and simplicity, submicrogram sensitivities remain a challenge [20].

The limitations imposed by the low analyte vapor pressure described above are also overcome through liquid-based dissolution. CE offers advantages for inorganic explosives screening due to the high solubility (in water) of inorganic ions. Additionally, CE with conductivity detection is widely used for direct analysis of inorganic ions [21], with extensive use of capacitively coupled contactless conductivity detection (C^4D) for portability and ease-of-use considerations [22–26]. Critical work towards portable inorganic oxidizer detection employing CE with C^4D was performed by Blanco et al. using a sequential injection CE instrument, built in-house with commercial components, for the separation of 10 inorganic anions within 90 s and detection limits $\leq$50 μg/L [27].

In most checkpoint screening and fieldable sampling scenarios, standard operating procedures employ a wipe-based sample collection of particulate and residue species from surfaces (e.g. suitcases, packages, cargo, persons, etc.). A commercial CE system based on microfluidic technology with indirect fluorescence detection has been applied to both wipe-based [28] and vapor [29] sampling for organic explosives. However, limitations for a fully automated method include the use of a wipe cutting and manual buffer addition for sample dissolution. Recent developments sought to couple a complimentary upstream sampling method with CE for direct chemical screening (GreyInnovation, greyscandetection.com)[1] [27]. The swipe collection from a surface is followed by automated dissolution and extraction to remove the collected sample for downstream detection. This directly parallels the subsequent thermal desorption process following wipe-based sample collection in traditional IMS screening platforms.

Here, we report on the investigation of an emerging CE-based commercial instrument utilizing C^4D (GreyScan ETD-100) for rapid, high-throughput screening of inorganic oxidizer-based explosives. The system demonstrated detection of oxidizers from complex fuel-oxidizer mixtures, including, propellants (e.g. BPs and black powder substitutes (BPS)) and pyrotechnics (e.g. flash powder-based firecracker). Related substances of neat target oxidizers (nitrate, chlorate, and perchlorate) were employed to evaluate system sensitivity and response based on spatial distribution of analyte along sampling wipes (i.e. "sweet spot" determination). The system response to variable mass distributions (i.e. arrays of low mass deposits versus a single equivalent deposit) and use of alternative wipe materials was also investigated. Finally, system stability as it pertained to screening arenas, including, sample carryover and baseline background considerations, was explored.

1 Materials and methods

2.1 Chemicals

All chemicals were purchased from Sigma-Aldrich (St. Louis, MO, USA) unless noted otherwise. Stock solutions of $KClO_3$, $KClO_4$, and KNO_3 were gravimetrically prepared in Chromasolv grade water to 25.4, 9.82, and 20.77 mg/mL, respectively. Samples were deposited onto wipes using these stock solutions by inkjet printing. BGE and elution buffer solutions were supplied with the GreyScan ETD-100 instrument from GreyInnovation (Melbourne, Australia). Acetate paper and Nomex meta-aramid wipes were purchased from Smiths Detection (Edgewood, MD, USA), and PTFE-coated fiberglass wipes were purchased from DSA Detection (North Andover, MA).

Various BPs, Goex BP FFFg and Elephant Supreme BP FFFg, and BPS, Blackhorn 209, Triple Seven FFFg, Pyrodex RS, and Jim Shockey's Gold, were provided by the U.S. Bureau of Alcohol, Tobacco, Firearms, and Explosives (ATF) Forensic Science Laboratory (Ammendale, MD, USA). A sample was also prepared using a Super Cobra 6 firecracker obtained from the Netherlands Forensic Institute containing $KClO_4$/aluminum flash powder with a BP primer. All BP and BPS samples, except Blackhorn 209, were prepared as

[1] Certain commercial equipment, instruments, or materials are identified in this article in order to specify the experimental procedure adequately. Such identification is not intended to imply recommendation or endorsement by NIST, nor is it intended to imply that the materials or equipment identified are necessarily the best available for the purpose.

1 mg/mL aqueous solutions and pipette-deposited onto acetate paper wipes for analysis. Deposited aqueous solutions were dried onto wipes (evaporation of solvent) for a total mass of 6 μg for Pyrodex RS and 3 μg for all other samples. Blackhorn 209 was crushed with a mortar and pestle prior to analysis as solid particulate. A sample from the Super Cobra 6 firecracker was collected by wiping the inside of the cardboard firework tube and analyzed as solid particulate.

2.2 Precision inkjet sample deposition

Wipe samples of $KClO_3$, $KClO_4$, and KNO_3 were prepared using a customized Jetlab 4 XL-B drop-on-demand piezoelectric inkjet printer [30,31] (MicroFab Technologies, Plano, TX, USA) in conjunction with published techniques [32]. A driving sine waveform, adjusted to match the rheological properties of the printing solvent (nominal period and dwell voltage of 85 μs and 32 V, respectfully), was used to eject discrete bursts of droplets from a MJ-AB-01-50-8MX dispensing device (MicroFab Technologies, Plano) with a 50 μm diameter orifice.

Sample solutions were deposited onto the wipes with the desired mass distributed at a single position (1 × 1) or as an array (2 × 2, 3 × 3, 4 × 4, and 7 × 7) to reach the desired total mass of sample. A 1.0 mm spot-to-spot spacing was maintained for printed sample arrays. Printing scripts were applied with normalized coordinates to match various positions of interest along the wipe coordinate grid. Inkjet spots were deposited in single bursts of droplets, ranging from (10 to 525) drops/burst, to achieve the desired total mass of deposited sample. Droplet masses were measured gravimetrically prior to and directly following sample printing using a SE2-F integrated microbalance (Sartorius Group, Bohemia, NY, USA) and evaluated for consistency. The average mass/droplet generally maintained a relative standard deviation no greater than 1%.

2.3 Capillary electrophoresis

A portable GreyScan ETD-100 CE instrument (GreyInnovation) was utilized for targeted screening of nitrates, chlorates, and perchlorates (greyscandetection.com). The CE instrument was 48.8 × 38.6 × 22.9 cm (width × depth × height) in size and weighed 13.1 kg. The instrument was equipped with a battery supply capable of (1 to 8) h of operation or, alternatively, was configurable for outlet power 100 to 240 V AC. Initial powering on of the instrument required a 10-min startup delay.

The GreyScan ETD-100 system incorporated a wipe-based sample introduction interface complementary to commercially available acetate paper wipes (Smiths Detection). Once a wipe was inserted into the instrument, a mechanical plunger sealed around the target collection area of the wipe and ran 200 μL of an elution solvent over the wipe for 5 s, from the inlet port to the outlet port. Extracted samples were then filtered for particulate prior to injection. Following sample extraction from the wipe, a 1.2 s pressure injection drove 15 nL of the sample into the capillary (25 μm i.d., 30 cm in length) for electrophoretic separation and detection using C^4D. The targeted nature of this portable CE instrument for inorganic anions allowed for 40 s run times. However, an additional (2 to 3) min was necessary to rinse the capillary after positive target analyte detection. Blank wipes containing no analyte were run every two or three samples, unless noted otherwise. Peak identification and normalization were achieved using three internal standard (IS) species and the system firmware. Comprehensive information regarding the buffers, ISs, and detection algorithms were proprietary.

The GreyScan ETD-100 system firmware was used for peak searching, peak identification, and peak height determination, unless otherwise noted. The measured conductivity signal and peak heights were normalized to the ISs and reported in digital units (du). Under typical operating conditions, an alarm algorithm is applied based on manufacturer-defined thresholds for detection. For this study, however, the processed data were exported and manually compiled. In addition, for limit of detection determinations, electropherograms were exported and processed using a custom MATLAB-based code (MATLAB R2019a, Mathworks Inc., MA, USA) for peak identification and height determination.

3 Results and discussion

The GreyScan ETD-100 CE instrument is a fully enclosed and automated inorganic-based explosives detection platform. Once the user inserts a sample wipe the following protocols are performed: sample extraction from the wipe, filtration of the extracted sample, CE separation and C^4D detection of the injected sample, waste of the unused elution and extraction solutions, and analysis of the resultant data against internal algorithms for the targeted identification of nitrates, chlorates, and perchlorates. The simplified user-directed interface allows for the option to run a sample and monitor instrument consumables.

3.1 Powder, propellant, and pyrotechnic fuel-oxidizer mixtures

Various propellant BP, BPS, and pyrotechnic flash powder fuel-oxidizer mixtures were analyzed, and representative electropherograms are shown in Fig. 1. Overall migration order for the target analytes, ISs, and background peaks was the following: chloride, nitrate, chlorate, acetate, perchlorate, IS 1 (IS1), carbonate, and IS 2 (IS2). Acetate and carbonate were identified as background peaks correlating to the sample wipe (acetate) and surrounding operational environment (carbonate). Chloride, IS1, and IS2 were incorporated for normalization (IS1, IS2) and background (Cl^-) with the buffers used.

Detection of the target oxidizer species (nitrates and perchlorates) exhibited no detrimental effects, such as peak

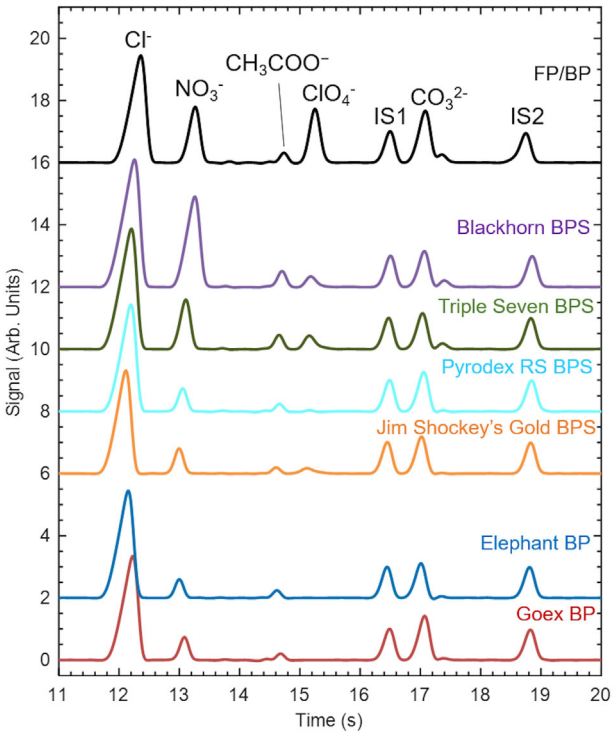

Figure 1. Representative electropherograms from flash powder (FP), black powder substitutes (BPS), and black powder (BP) samples. Data shifted vertically for visualization. Peaks represent chloride (Cl^-), nitrate (NO_3^-), acetate (CH_3COO^-), internal standard 1 (IS1), carbonate (CO_3^{2-}), and internal standard 2 (IS2).

shifts or interfering peaks, from the additional components in these mixtures. A previous mass spectrometry analysis was used to verify the contents of these samples [33]. Unfortunately, the targeted nature and limited elution window of the system prohibited the detection of any of the other organic and inorganic fuels and oxidizers. For example, the nitrate component of the BPs, a simple mixture of potassium nitrate, sulfur, and charcoal, was clearly identified. However, no resulting sulfur-based anions were detected within the predefined elution window. Nitrate was successfully detected in all seven samples, and this was presumed to be from the potassium nitrate oxidizer component of these samples. However, in the case of the Blackhorn 209 BPS, the organic oxidizer guanidine nitrate likely contributed to the strong nitrate signal. BPS formulations were developed to provide better performance than traditional BPs. These formulations often include potassium perchlorate and other organic and inorganic fuels and oxidizers. Perchlorate was successfully detected in all BPS samples and the flash powder-based firecracker (Fig. 1). However, none of the additional organic and inorganic components known to be present in the sample were observed within the limited window, for example, ascorbic acid (Jim Shockey's Gold), sodium benzoate (Pyrodex and Triple Seven), dicyandiamide (Pyrodex and Triple Seven), 3-nitrobenzoic acid (Triple Seven), or aluminum (firecracker). Although targeted detection enabled rapid analysis times for the selected analytes, minimal differentiation of these related propellants and pyrotechnics were observed. As expected, no chlorate was observed for all seven samples, and perchlorate was only observed in the BPS samples.

The specific detection application and wipe availability can impact end-user preference for selecting a wipe material. For example, if the end-user desires a wand sampling method for wipe handling, or an emphasis on sample collection efficiencies, each of these factors might alter wipe material selection. Additionally, cost per wipe and reusability contributes to these considerations. The ability to use common commercial wipes other than the acetate paper wipes provided with the GreyScan ETD-100 instrument was evaluated. Frequently used wipes for explosives detection include PTFE-coated fiberglass weaves and nonwoven meta-aramid wipes. Both PTFE-coated fiberglass and meta-aramid wipes showed no additional background peaks correlating to the wipe material, however, peak shifting in the migration time for chloride was observed (Supporting information Fig. S1A). Additionally, poor reproducibility was observed with the PTFE-coated fiberglass and meta-aramid wipes. This was likely due to the vertical wipe insertion and complementary plunger mechanism for automated sample extraction, limiting the use to the acetate paper-based wipes (Supporting information Fig. S1B).

3.2 Standard Response and Sensitivities of ClO_3^-, ClO_4^-, and NO_3^-

Inkjet printing was utilized as a precise method for depositing potassium chlorate, potassium perchlorate, and potassium nitrate onto acetate wipes to determine detection limits. Using a highly reproducible test material is key to verifying measurement results and methods for new systems. Only a portion of the wipe was inserted into the instrument, and a 3D rendering of the instrument-wipe interface is shown in Fig. 2A. The inlet port is used to introduce extraction buffer for sample dissolution from the wipe, and the outlet port used to collect the extracted sample for downstream processing. Both ports were offset along the edges of a circular mechanically-actuated plunger. The wipe surface that contacts this plunger was considered the target sample collection area. To prepare sample wipes for analysis, the analyte solution was inkjet-printed as a single spot at the corresponding center position between the inlet and outlet ports. The wipe-based inkjet printing coordinates (in millimeters) are described in Fig. 2B with the center position (13, 20) denoted.

Instrument sensitivities with inkjet-printed wipes were empirically determined in accordance with ASTM E2677 [34] using limits of detection (LOD_{90}) that correspond to the lowest detectable mass with 90% probability of true detection. Target analyte wipes were fabricated by depositing the appropriate number of droplets from stock solutions to provide 0, 10, 30, 100, 300, and 1000 ng total mass of printed analyte. Calibration curves were obtained using peak heights from 10 replicate wipes for each analyte mass to generate LOD_{90} and

Table 1. Targeted detection peaks for nitrate, chlorate, and perchlorate

Target analyte	Migration time (s)	LOD_{90} (ng)	90% Upper confidence limit (ng)	Response curve linearity (R^2)	FWHM (s)
Nitrate	12.98 ± 0.12	198.1	284.2	0.99	0.19 ± 0.06
Chlorate	13.53 ± 0.11	71.9	130.4	0.96	0.17 ± 0.02
Perchlorate	15.12 ± 0.06	146.5	257.6	0.90	0.19 ± 0.03

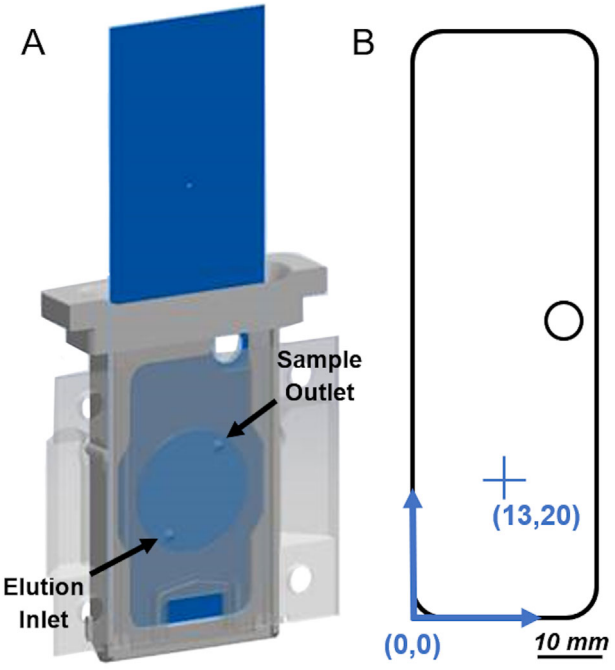

Figure 2. (A) 3D rendering for a surface wipe (blue) within the wipe insertion apparatus (gray) on the GreyScan CZE Instrument (ETD-100) with elution solvent inlet and liquid-extracted sample outlet ports denoted. (B) Schematic of the acetate paper surface wipe with target collection area center point (13, 20) between the inlet and outlet extraction ports denoted using a wipe-based coordinate grid with millimeter units.

correlation (R^2) values. Processed electropherograms (normalized to ISs) were exported from the instrument and used to measure migration times and peak heights for each target analyte. Of the three analytes, chlorate resulted in the lowest calculated LOD_{90} at 71.9 ng and nitrate resulted in the highest LOD_{90} at 198.1 ng (Table 1). Migration order of the target analytes was nitrate, chlorate, and perchlorate with migration times shown in Table 1. Migration times for each analyte exhibited less than 1% relative standard deviation (RSD), providing a reproducible method for peak identification using migration time (Supporting information Fig. S2). Migration times and full width at half maximum (FWHM) average and standard deviations were calculated using all replicate runs that exhibited analyte peaks (n = 52 perchlorate, n = 70 chlorate, n = 93 nitrate).

Within each resultant electropherogram, the chloride background peak eluted first and the ISs (IS1, IS2) eluted after the target analytes. The ISs were added to the sample prior to sample injection and separation, however, chloride was present in the extraction buffer allowing for detectable signal variabilities due to the extraction process. The LOD_{90} for each target analyte was also calculated using a ratio of the target analyte peak height to the chloride peak to account for variability in signal intensities between runs. An improvement in the normalized ratio LOD_{90} values was observed, specifically, 14.3, 6.6, and 5.9% for nitrate, chlorate, and perchlorate, respectively (Supporting information Table S1). Applying signal normalization with chloride accounted for factors that could affect extraction efficiencies. Variabilities arise from sample heterogeneity in the extracted aliquot, inconsistencies in the position of the wipe, and unintentional folding of the wipe during insertion into the instrument. The system performance and variabilities due to the wipe-based sample introduction and automated extraction were explored next.

3.3 Spatial distribution of sample on wipes

Due to the offset position of the sample extraction inlet and outlet ports (Fig. 2A), the instrument response relative to the spatial distribution of analyte was investigated. Potassium chlorate was chosen as an exemplary target analyte to evaluate the spatial distribution of various deposition locations printed to total 300 ng. Single inkjet-printed analyte spots were oriented using coordinates overlaid with the wipe and are denoted in Fig. 3 as red circles for a total of 21 locations. The displayed surface plots were created using a triangulation-based cubic interpolation across a single millimeter level grid (MATLAB R2019a). The outer extent of the coordinate grid used, along (0, 0) to (0, 26) and (0, 26) to (26, 40), etc., is described in red in Supporting information Fig. S3A. Five replicate sample wipes were analyzed for the chlorate peak height, reported as signal intensity in digital units (du), at each location except the center position (13, 20), which included ten replicates. The printed coordinate grid is represented in Fig. 3 with the distance across and along the wipe plotted on the x- and y-axes to show the spatial distribution of the signal intensities or %RSD magnitudes represented in false color for visualization.

As indicated by the yellow color in Fig. 3A, the chlorate signal intensity increased as the deposited sample location approached the outlet port, used to withdraw the extracted sample solution for downstream processing. The highest signal intensities resulted from printed locations between coordinates (18, 25) and (18, 20). Additionally, printed locations

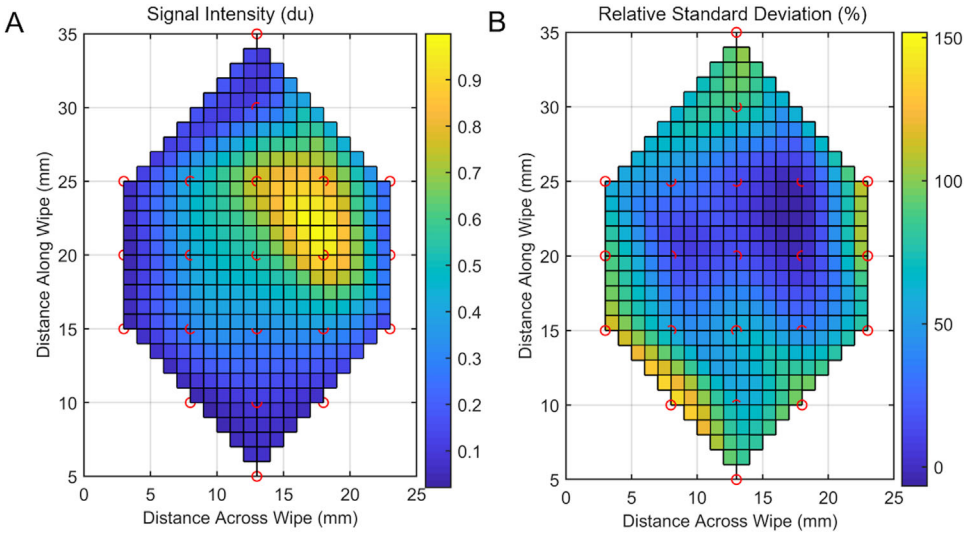

Figure 3. Printed 300 ng $KClO_3$ as an exemplary inorganic explosive onto the surface wipes to measure the optimal position for sample extraction using the Greyscan CE instrument. (A) Plot of the signal intensities superimposed and extrapolated onto the printed coordinate grid with red demarcations indicating true measurement coordinates. (B) Plot of the percent relative standard deviation (%RSD) of the peak intensities superimposed onto the printed coordinate grid with red demarcations indicating true measurement coordinates.

closest to the inlet port for introduction of the extraction buffer, towards coordinate (10, 10), exhibited decreased signal intensities. Fig. 3B shows the corresponding %RSD values for the average peak intensities in Fig. 3A. Similarly, the locations closest to the outlet port demonstrated the lowest %RSD and most reproducible results. Alternatively, locations towards the inlet port yielded inconsistent results with high %RSDs (yellow/lighter color). Given common swipe-based sample collection procedures, the spatial distribution can vary widely from sample-to-sample. However, modified wipes incorporating surface topography to localize collection locations towards the outlet port position and to concentrate samples might provide direct benefit here. In addition to the reduction in variability due to the spatial location of collected samples, localizing the sample could also enable a reduction in the necessary extraction buffer (i.e. 200 μL), effectively increasing the analyzed concentration. Although localization of sample could be advantageous, the variability of the wipe position observed upon insertion (approximately ± 1 mm) into the instrument due to the size of the insertion apparatus would need to be addressed. Factors, including the sample extraction buffer volume, implementation of an automated mixing protocol, delayed injection of sample to allow for further sample dissolution, and flow velocity over the wipe during the liquid-based extraction step could also impact the signal intensities and extraction efficiencies. Currently, no known sample preparation steps were utilized during sample extraction from the wipe to homogenize the sample solution or to facilitate rapid dissolution of sample for increased recoveries, for example, mixing or sonication. Implementation of additional sample processing steps could provide decreased variability in the signal response relative to the spatial distribution of collected sample and would require modification to the instrumentation or operational protocol.

The instrument response relative to analyte distribution was further investigated using various printed potassium chlorate arrays. The total mass of potassium chlorate, either 300 or 1000 ng, remained constant across various arrayed distributions, including arrays of 1 × 1, 2 × 2, 3 × 3, 4 × 4, and 7 × 7 printed spots (Supporting information Fig. S3B). For example, a 1000 ng, 2 × 2 array was printed as four 250 ng spots around the center coordinate position (13, 20) to total 1000 ng of potassium chlorate. Each array was printed around the center grid position with 1.0 mm spacing between the printed spots within the array. The discrete nature of the inkjet printing process (discrete # of drops per spot) resulted in an RSD of 1.8 and 0.5% for the 300 ng and 1000 ng total deposited mass, respectively. Five replicate wipes were analyzed for the average chlorate peak height, reported as signal intensities, for each array distribution (≥ 2 × 2) besides the 1 × 1 single point data collected over 15 replicate wipes. As shown in Fig. 4, all resultant signal intensities for each array distribution at both 300 and 1000 ng total mass, including 2 × 2, 3 × 3, 4 × 4, and 7 × 7, were within the 95% confidence interval bounds of the median signal response for the 1 × 1 single point results. Between the arrays, there were limited observable differences in the median signal intensities without a clear trend as the array size increased, likely due to the symmetric nature of the deposited arrays. For each spot closer to the sample outlet (yielding higher signal intensity), there was a corresponding spot further from the sample outlet (yielding lower signal intensity). Even though a portion of the outer printed spots of the 1000 ng 7 × 7 array were closer to the outlet port, there remained no observable improvement in signal response. Alternatively, a small increase in median signal was seen for the 300 ng 4 × 4 array, although the interquartile range also increased.

3.4 Baseline background levels and system stability

Blank wipes containing no analyte were run every 2 to 3 samples to investigate variations in background and possible

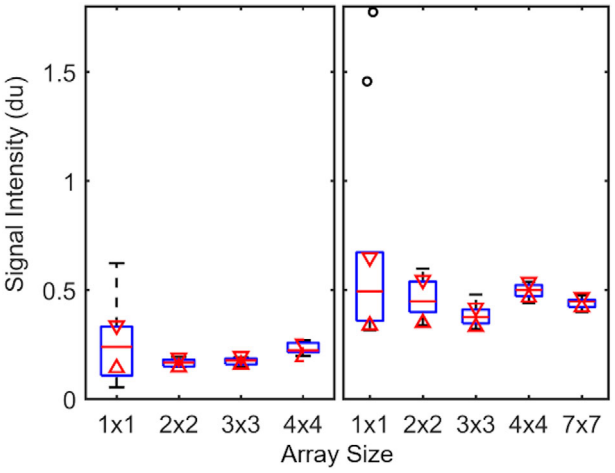

Figure 4. Plot of peak intensities for printed $KClO_3$ at 300 ng (left) and 1000 ng (right) at various array sizes compared to a single-point distribution (1 × 1). Boxes, whiskers, and outliers (o) represented by the median with lower and upper quartiles, 1.5 × the interquartile range, and values outside the whisker range, respectively. Intensities are normalized to the IS1 peak.

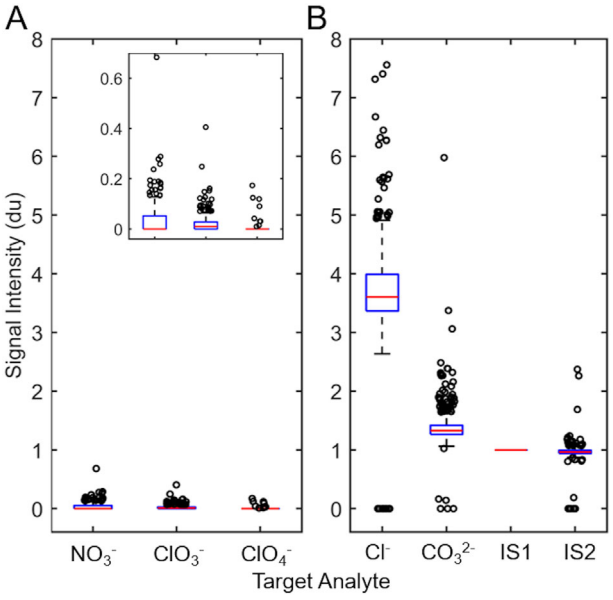

Figure 5. Plots of the baseline background (A) and system stability (B) from all analyses. (A) Box plot of peak intensities from blank wipes (n = 224) with no analyte to observe any sample carryover between target analyte runs for nitrate, chlorate, and perchlorate. (B) Box plot of peak intensities for background and internal standards from wipes with and without target analytes (n = 777) for chloride, carbonate, IS1, and IS2. Boxes, whiskers, and outliers (o) represented by the median with lower and upper quartiles, 1.5 × the interquartile range, and values outside the whisker range, respectively. Intensities are normalized to the IS1 peak.

analyte carryover after a single or successive positive target identification wipe(s). The plot in Fig. 5A summarizes the background peak intensities correlating to the migration times of the target analytes in all blank runs when no analyte was added to the acetate paper wipes prior to analysis. This data plot includes 224 replicate blanks analyzed intermittently between target analyte studies. Overall, the median value was 0 du for all three target analyte locations. The lowest background response was observed for perchlorate and the highest for nitrate with background signals of 0.002 ± 0.02 du and 0.04 ± 0.07 du, respectively (Supporting information Table S2). Using the derived calibration curves with LOD_{90} calculations, 1 wipe, 5 wipes, and 1 wipe for nitrate, chlorate, and perchlorate, respectively, out of the 224 blank wipes analyzed would be incorrectly identified. False positive rates due to background signal could be improved by using the 90% upper confidence limits, resulting in only 1 wipe, 3 wipes, and 1 wipe incorrectly identified for nitrate, chlorate, and perchlorate, respectively. Ultimately, these limited false positive results are not of major concern as the frequency of incorrect identification is easily manipulated by implementing and adjusting programmed thresholds into the instrument firmware. Reduction in the number of false positives is achieved by increasing a predetermined signal threshold, however, detection limits would also increase.

Additionally, 15 to 20 successive wipes at 100 ng and 1000 ng potassium chlorate loadings were run without intermittent blank wipes or the additional flush protocol performed after each positive result. All wipes produced a positive result that would normally trigger the flush protocol, however, these flush steps were overridden to investigate target analyte accumulation between samples. Even without these flush cycles, no significant carryover was observed (Supporting information Fig. S4). Overloaded wipes with much higher sample mass amounts collected than those analyzed here could be possible in some screening environments and may require additional flush protocols to be applied between each analyzed sample wipe.

The box plot in Fig. 5B shows the overall system stability utilizing the peak intensities of the ISs and background. This data included 777 sample runs over a 2-week period and included both blank wipes with no analyte added and wipes with various target analytes. All signal intensities were normalized by the system firmware relative to an IS1 intensity of 1.0 du. Overall, IS2 resulted in a stable and steady signal intensity over all runs, with a median value of approximately 1.0 du. Both IS1 and IS2 are added to the sample solution prior to separation and detection. Unlike IS1 and IS2, the chloride peak was influenced by inconsistencies in the sample extraction method, possibly due to heterogeneities in the extract solution, unintentional folding of the wipe during insertion, incomplete insertion of the wipe, and variability of the inserted wipe position, resulting in subtle changes in chloride concentration between analyses. The increased chloride peaks resulted from studies where blank wipes were not run intermittently between sample wipes. The increase in carbonate peak intensities correlated to the first samples run at the start of each day. Generally, no known impact was observed on analyses from ISs and background signal variations.

Finally, system stability and continuous operation were also dependent on the necessary filtration of unwanted fibrous and particulate species from entering the separation capillary. Scanning electron microscope (SEM) images of the filter-collected materials exhibited fibers, fibrous materials, and other particulate clearly larger than the 25 μm capillary inner diameter (Supporting information Fig. S5). These isolated contaminants were likely collected from various sampling surfaces, particulate samples, or alternative wipes, which included cardboard boxes, cardboard firework tubes, plastic bags, bag labels, packaging tape, and nitrile gloves. Filter replacement notifications were provided to the user through the system firmware.

4 Concluding remarks

The portable GreyScan ETD-100 CE instrument was used as an inorganic-based explosives detection technique for targeted analysis of common inorganic anions, for example, chlorate, perchlorate, and nitrate. These target oxidizers were correctly identified from mixtures containing a wide range of organic and inorganic fuels. Sensitive detection of <200 ng was demonstrated for the target analytes, however, a collection localization scheme complimentary to the automated extraction mechanism could improve detection capabilities. Regions for optimal sample extraction "sweet spots" on the collection wipes were identified using inkjet printing for precise spatial distribution of analyte along the wipe material. The position of the sweet spot correlated with the extracted sample outlet within the wipe insertion apparatus. Utilizing surface topography-modified wipes to focus and concentrate sample collection towards a localized position correlating to the sample outlet port could improve detection sensitivity. Additionally, normalization of the signal to the chloride peak also showed improvement in the detection limits, accounting for variabilities in the sample extraction procedure. Overall, minimal carryover was observed across all experiments and the expected run time per sample is 40 s with an additional (2-3) min with positive identification. Further considerations in instrument portability could be explored, and many groups have utilized microfluidic electrophoresis coupled with C^4D for the detection of relevant compounds for wipe-based sampling, e.g., illicit drugs [35,36]. However, a decrease in sensitivity could result using a microfluidic platform due the fast migration of inorganic anions [37]. Alternative electrophoresis methods could be explored to overcome challenges in detection sensitivity [38].

The U.S. Department of Homeland Security Science and Technology Directorate sponsored a portion of the production of this material under Interagency Agreement IAA FTEN-18-00014 with the National Institute of Standards and Technology. The authors would like to thank Matt Porter, Susan Hallowell, and Doug Freitag at GreyScan Detection for informative discussion and providing the wipe insertion schematic; Cindy Wallace at the Bureau of Alcohol, Tobacco, Firearms, and Explosives for providing the black powders and black powder substitutes; as well as Karlijn Bezemer and Arian van Asten at the Netherland Forensic Institute for providing the firecracker test samples. This research was performed while S.T.K. held a National Institute of Standards and Technology (NIST) National Research Council (NRC) Research Postdoctoral Associateship Award. Official contribution of the National Institute of Standards and Technology; not subject to copyright in the United States.

The authors have declared no conflict of interest.

5 References

[1] United States Bomb Data Center (USBDC), 2018 Explosives Incident Report (EIR). 2018 Explosives Incident Report. https://www.atf.gov/explosives/docs/report/2018-explosives-incident-report-eir (accessed September 2019).

[2] Klunder, G. L., Grant, P. M., Andresen, B. D., Russo, R. E., *Anal. Chem.* 2004, *76*, 1249–1256.

[3] Chen, J., Shi, Y. E., Zhang, M., Zhan, J. H., *RSC Adv*. 2016, *6*, 51823–51829.

[4] Hakonen, A., Andersson, P. O., Schmidt, M. S., Rindzevicius, T., Kall, M., *Anal. Chim. Acta* 2015, *893*, 1–13.

[5] Yu, W. W., White, I. M., *Analyst* 2013, *138*, 1020–1025.

[6] Zhang, R., Xu, B. B., Liu, X. Q., Zhang, Y. L., Xu, Y., Chen, Q. D., Sun, H. B., *Chem. Commun.* 2012, *48*, 5913–5915.

[7] Lee, C. H., Tian, L. M., Singamaneni, S., *ACS Appl. Mater. Interfaces* 2010, *2*, 3429–3435.

[8] Gong, Z. J., Wang, C. C., Wang, C., Tang, C. Y., Cheng, F. S., Du, H. J., Fan, M. K., Brolo, A. G., *Analyst* 2014, *139*, 5283–5289.

[9] Gong, Z. J., Du, H. J., Cheng, F. S., Wang, C., Wang, C. C., Fan, M. K., *ACS Appl. Mater. Interfaces* 2014, *6*, 21931–21937.

[10] Woodfin, R. L. (Ed.), *Trace Chemical Sensing of Explosives*, John Wiley & Sons, New Jersey 2007, pp 3–34.

[11] Staymates, M. E., MacCrehan, W. A., Staymates, J. L., Kunz, R. R., Mendum, T., Ong, T. H., Geurtsen, G., Gillen, G. J., Craven, B. A., *Sci. Rep.* 2016, *6*, 36876.

[12] Yinon, J., *TrAC Trends Anal. Chem*. 2002, *21*, 292–301.

[13] Najarro, M., Morris, M. E. D., Staymates, M. E., Fletcher, R., Gillen, G., *Analyst* 2012, *137*, 2614–2622.

[14] Liang, X. X., Zhou, Q. H., Wang, W. G., Wang, X., Chen, W. D., Chen, C., Li, Y., Hou, K. Y., Li, J. H., Li, H. Y., *Anal. Chem.* 2013, *85*, 4849–4852.

[15] Peng, L., Hua, L., Wang, W., Zhou, Q., Li, H., *Sci. Rep.* 2014, *4*, 6631.

[16] Kelley, J. A., Ostrinskaya, A., Geurtsen, G., Kunz, R. R., *Rapid Commun. Mass Spectrom.* 2016, *30*, 191–198.

[17] Forbes, T. P., Sisco, E., Staymates, M., Gillen, G., *Anal. Methods* 2017, *9*, 4988–4996.

[18] Forbes, T. P., Staymates, M., Sisco, E., *Analyst* 2017, *142*, 3002–3010.

[19] Forbes, T. P., Sisco, E., Staymates, M., *Anal. Chem.* 2018, *90*, 6419–6425.

[20] Peters, K. L., Corbin, I., Kaufman, L. M., Zreibe, K., Blanes, L., McCord, B. R., *Anal. Methods* 2015, *7*, 63–70.

[21] Calcerrada, M., González-Herráez, M., García-Ruiz, C., *TrAC Trends Anal. Chem.* 2016, *75*, 75–85.

[22] Kuban, P., Hauser, P. C., *TrAC Trends Anal. Chem.* 2018, *102*, 311–321.

[23] Van Schepdael, A., *Separations* 2016, *3*, 2.

[24] Zhang, M., Phung, S. C., Smejkal, P., Guijt, R. M., Breadmore, M. C., *Trends Environ. Anal. Chem.* 2018, *18*, 1–10.

[25] Kobrin, E. G., Lees, H., Fomitsenko, M., Kuban, P., Kaljurand, M., *Electrophoresis* 2014, *35*, 1165–1172.

[26] Hutchinson, J. P., Johns, C., Breadmore, M. C., Hilder, E. F., Guijt, R. M., Lennard, C., Dicinoski, G., Haddad, P. R., *Electrophoresis* 2008, *29*, 4593–4602.

[27] Blanco, G. A., Nai, Y. H., Hilder, E. F., Shellie, R. A., Dicinoski, G. W., Haddad, P. R., Breadmore, M. C., *Anal. Chem.* 2011, *83*, 9068–9075.

[28] Ueland, M., Blanes, L., Taudte, R. V., Stuart, B. H., Cole, N., Willis, P., Roux, C., Doble, P., *J. Chromatogr. A* 2016, *1436*, 28–33.

[29] Taranto, V., Ueland, M., Forbes, S. L., Blanes, L., *J. Chromatogr. A* 2019, *1602*, 467–473.

[30] Verkouteren, R. M., Verkouteren, J. R., *Anal. Chem.* 2009, *81*, 8577–8584.

[31] Verkouteren, R. M., Verkouteren, J. R., *Langmuir* 2011, *27*, 9644–9653.

[32] Verkouteren, J. R., Lawrence, J., Klouda, G. A., Najarro, M., Grandner, J., Verkouteren, R. M., York, S. J., *Analyst* 2014, *139*, 5488–5498.

[33] Forbes, T. P., Verkouteren, J. R., *Anal. Chem.* 2019, *91*, 1089–1097.

[34] Standard Test Method for Determining Limits of Detection in Explosive Trace Detectors, ASTM International, 2014. https://www-s.nist.gov/loda/

[35] Moreira, R. C., Costa, B. M. C., Marra, M. C., Santana, M. H. P., Maldaner, A. O., Botelho, E. D., Paixao, T., Richter, E. M., Coltro, W. K. T., *Electrophoresis* 2018, *39*, 2188–2194.

[36] Tai, C. T., See, H. H., *Electrophoresis* 2019, *40*, 455–461.

[37] Pinheiro, K. M. P., Moreira, R. C., Rezende, K. C. A., Talhavini, M., Lograd, L. P. L., Baio, J. A. F., Lanza, M. R. V., Coltro, W. K. T., *Electrophoresis* 2019, *40*, 462–468.

[38] Flanigan, P. M., Ross, D., Shackman, J. G., *Electrophoresis* 2010, *31*, 3466–3474.

